Atmospheric Environment 104 (2015) 39–49

Contents lists available at ScienceDirect

Atmospheric Environment

journal homepage: www.elsevier.com/locate/atmosenv

Lung burden and deposition distribution of inhaled atmospheric urban ultrafine particles as the first step in their health risk assessment

Imre Salma [a, *], Péter Füri [b], Zoltán Németh [a], Imre Balásházy [b], Werner Hofmann [c], Árpád Farkas [b]

[a] Institute of Chemistry, Eötvös University, H-1518 Budapest, P.O. Box 32, Hungary
[b] Centre for Energy Research, Hungarian Academy of Sciences, H-1525 Budapest, P.O. Box 49, Hungary
[c] Department of Materials Research and Physics, University of Salzburg, A-5020 Salzburg, Hellbrunnerstr. 34, Austria

HIGHLIGHTS

- Deposition fractions of inhaled particles in the human respiratory tract are ca. 56%.
- Deposition rates in the lung (up to 10^9 particles min^{-1}) are larger than in the extra-thoracic region.
- Deposition rate in the acinar region increases by physical activity.
- The extra-thoracic region receives the largest surface density deposition rates (up to 10^6 particle cm^{-2} min^{-1}).
- In the lung, the first few airway generations obtain the highest surface loading (up to 10^5 particle cm^{-2} min^{-1}).

ARTICLE INFO

Article history:
Received 9 September 2014
Accepted 23 December 2014
Available online 2 January 2015

Keywords:
Exposure assessment
Respiratory deposition
Surface density deposition
Nanoaerosol
Stochastic lung deposition model

ABSTRACT

Realistic median particle number size distributions were derived by a differential mobility particle sizer in a diameter range of 6–1000 nm for near-city background, city centre, street canyon and road tunnel environments in Budapest. Deposition of inhaled particles within airway generations of an adult woman was determined by a stochastic lung deposition model for sleeping, sitting, light and heavy exercise breathing conditions. Deposition fractions in the respiratory tract were considerable and constant for all physical activities with a mean of 56%. Mean deposition fraction in the extra-thoracic region averaged for the urban environments was decreasing monotonically from 26% for sleeping to 9.4% for heavy exercise. The mean deposition fractions in the tracheobronchial region were constant for the physical activities and urban environments with an overall mean of 12.5%, while the mean deposition fraction in the acinar region averaged for the urban locations increased monotonically with physical activity from 14.7% for sleeping to 34% for heavy exercise. The largest contribution of the acinar deposition to the lung deposition was 75%. The deposition rates in the lung were larger than in the extra-thoracic region, and the deposition rate in the lung was increasingly realised in the AC region by physical activity. It was the extra-thoracic region that received the largest surface density deposition rates; its loading was higher by 3 orders of magnitude than for the lung. Deposition fractions in the airway generations exhibited a distinct peak in the acinar region. The maximum of the curves was shifted to peripheral airway generations with physical activity. The shapes of the surface density deposition rate curves were completely different from those for the deposition rates, indicating that the first few airway generations received the highest surface loading in the lung.

1. Introduction

Ultrafine (UF) atmospheric aerosol particles (with an equivalent diameter <100 nm) are usually present in large number concentrations (daily medians up to 10^4–10^5 cm^{-3}) and abundances

* Corresponding author.
E-mail address: salma@chem.elte.hu (I. Salma).

http://dx.doi.org/10.1016/j.atmosenv.2014.12.060
1352-2310/

(70%–90% of all aerosol particles) in cities (Kulmala et al., 2004; Aalto et al., 2005; Putaud et al., 2010; Borsós et al., 2012). They are emitted directly from high-temperature sources or they are formed in the air by atmospheric nucleation. Nanotechnology and its products such as engineered nanoparticles can play an important role in workplace or indoor environments. Inhalation of UF particles can represent an excess health risk relative to coarse or fine particles of the same or similar chemical composition (Oberdörster et al., 2005; Kreyling et al., 2006; HEI Review Panel, 2013). The specific effects are mainly associated with the large number of insoluble particles deposited in the respiratory system, their large total surface area and their very small size (Yang et al., 2008; Carvalho et al., 2011; Braakhuis et al., 2014). There is increasing scientific evidence that removal of particles deposited in the lung is also size-specific. The smallest UF particles, i.e., the nanoparticles (with an equivalent diameter <10 nm) deposited in the deep airways are less efficiently phagocytised by alveolar macrophages and epithelial cells than larger particles (Geiser et al., 2005; Oberdörster et al., 2005). In the bronchial region, the fraction of particles cleared up by the mucociliary escalator is also decreasing as their size decreases (Kreyling et al., 2006). Due to the increased retention times, the deposited insoluble ultrafine particles can accumulate in and damage the lung (e.g., by inducing inflammatory injury or oxidative stress) or may cross the cellular membrane barrier of the respiratory epithelium (Geiser et al., 2005) entering into the blood circulation or the lung-associated lymph nodes. This may result in the systematic translocation of deposited insoluble nanoparticles to other organs (Yang et al., 2008). The clearance from these secondary organs is very low in general (Kreyling et al., 2002; Geiser et al., 2008), and therefore, accumulation can occur also in these organs. Implications of the possible lung overload by and accumulation of UF particles in healthy humans are inconclusive (Oberdörster et al., 2005; Braakhuis et al., 2014). The related uncertainties can be decreased by risk assessment studies on UF aerosol. For these reasons, more information on both the human exposure to UF particles (including their deposition and clearance) and on the toxicity hazard of the deposited particles is required (Nel et al., 2006).

Several research studies were devoted to physical and chemical characterisation of UF aerosol in cities (e.g., Wehner and Wiedensohler, 2003; Aalto et al., 2005; Harrison and Jones, 2005; Jeong et al., 2006; Qian et al., 2007; Rodríguez et al., 2007; Avino et al., 2011; Reche et al., 2011; Salma et al., 2011a, 2014; Dall'Osto et al., 2013). It was concluded that 1) temporal variation of the particle number concentration can be up to 2 orders of magnitude in central urban sites; 2) daily average particle number concentration in near-city background and high-traffic urban locations can vary by a factor of up to 40; and 3) median particle diameters decrease with the anthropogenic impact (more exactly with fresh vehicle emissions). Despite the coincidence of the high particle number concentrations and high population in large cities, there is limited information available on the long-term inhalation exposure of the public to atmospheric urban aerosol with respect to particle numbers.

In the present study, deposition of realistic polydisperse atmospheric aerosol particles expressed by particle number concentrations in the respiratory system of an adult woman performing reference levels of physical activity in four different types of urban environment within a city is investigated by using a whole respiratory system particle deposition model. The main objectives are to report the relevant aerosol properties for modelling, to discuss the capabilities of an advanced stochastic lung deposition model for urban nanoparticles, to determine representative particle deposition metrics, to explain the derived properties, and to interpret the exposure results.

2. Methods

2.1. Measuring system

Atmospheric aerosol particles were measured by a flow-switching type differential mobility particle sizer (DMPS) (Salma et al., 2011a). The system operates in an electrical mobility diameter range from 6 to 1000 nm in 30 size channels at two sets of flows. In the first flow mode, 20 size channels are measured (from 6 to 200 nm), while in the second flow mode, 10 size channels are acquired (from 200 to 1000 nm). The diameters obtained refer to the dry state of particles with a typical relative humidity (RH) < 20%. The measurements were performed with a time resolution of approximately 10 min. The measuring system and method fulfil the recommendations of the international technical standards (Wiedensohler et al., 2012).

2.2. Measurement sites and time intervals

The measurements were performed in Budapest (Hungary) in four different urban environments, i.e., in near-city background, city centre, street canyon and traffic (road tunnel) microenvironments (Salma et al., 2014). The measurements in the near-city background were performed on the western border of the city within a wooded area (latitude 47° 30′ 1.4″ N, longitude 18° 57′ 46.3″ E, altitude 478 m above sea level, a.s.l.) continuously from 18 January 2012 to 17 January 2013. The location is expected to represent the air masses entering the city since the prevailing wind direction is NW. The measurements in the city centre were accomplished in District Lágymányos (latitude 47° 28′ 29.8″ N, longitude 19° 03′ 44.6″ E, altitude 114 m a.s.l.) continuously from 3 November 2008 to 2 November 2009 (Salma et al., 2011a). The location usually receives well-mixed air masses directly from the city centre. The measurements in the street canyon were performed in Rákóczi Street (latitude 47° 29′ 39.4″ N, longitude 19°03′ 36.3″ E, altitude 111 m a.s.l) continuously from 28 March to 31 May 2011. The street is situated in the city centre, and belongs to regular long street canyons. The measurements in the traffic microenvironment were carried out in the Castle District Tunnel (latitude 47° 29′ 54.5″ N, longitude 19° 02′ 24.6″ E, altitude 106 m a.s.l. at its eastern gate) continuously from 12 to 26 July 2010 (Salma et al., 2011b). The tunnel is situated in the city centre, has a single, straight bore with a length of 350 m, and comprises two-lane road traffic. These environments represent ordinary conditions for European cities.

2.3. Treatment of experimental data

Median particle number concentrations for each size channel were obtained from the measured 10-min normalised particle number concentration data ($\Delta N/\Delta \log d$, where N is the particle number concentration and d is the particle equivalent diameter) for the whole measuring time intervals, and these were utilised for deriving median particle number size distributions. The DMPS measures electrical mobility diameter (d_{mob}) of particles. Diffusion (Brownian motion), inertial impaction and sedimentation (gravitational settling) are the basic deposition mechanisms of inhaled aerosol particles in the human respiratory tract. Diffusion becomes the dominant deposition mechanism for particle sizes below approximately 100 nm, and it is related mainly to mobility diameter. Therefore, the size distributions were first expressed in this measured diameter. At the same time, inertial impaction and sedimentation become the controlling deposition mechanisms above 1 μm, and they are associated with aerodynamic diameter (d_a) of particles. For this reason, the size distributions were also expressed in aerodynamic diameter representation. Diameters d_{mob}

were converted to d_a using the following approach (DeCarlo et al., 2004; Khlystov et al., 2004; Ondráček et al., 2009):

$$d_a = \sqrt{\frac{\rho_p}{\rho_0}\frac{1}{\chi}\frac{C_c(d_{ve})}{C_c(d_a)}}d_{ve}\,, \qquad (1)$$

where d_{ve} is the volume equivalent diameter, ρ_p and ρ_0 are the particle density and unit density ($\rho_0 = 1$ g cm^{-3}), χ is the dynamic shape factor of the particle, and $C_c(d)$ is the slip correction factor for the particle with a diameter of d. It was assumed that the particles have a spherical shape, which implies that $\chi = 1$ by definition, and that $d_{ve} = d_{mob}$. It was observed earlier that the effective density of agglomerated UF (diesel exhaust or soot) particles has a decreasing tendency due to the increased abundance of organic non-volatile components and adsorbed volatile organic species from about 1.78 g cm^{-3} (bulk material density) above 220 nm to 1.27 g cm^{-3} at 50 nm, and to 0.65 g cm^{-3} (similar to carbon black) at 10 nm with a levelling off at smaller diameters (Park et al., 2004; Giechaskiel et al., 2009; Rissler et al., 2013). Deviations in the effective density can happen depending on the actual source types of the primary particles, extent of their agglomeration, and burning conditions. Nevertheless, the listed assumptions are all reasonable and acceptable for the atmospheric UF particles and secondary atmospheric urban particles under ordinary ambient environmental conditions in the diameter range considered. To obtain the size distributions in terms of aerodynamic diameters, the normalised concentration data were also converted from $\Delta\log d_{mob}$ to $\Delta\log d_a$. Number median mobility diameters (NMMDs), number median aerodynamic diameters (NMADs) and geometric standard deviations (GSDs) were determined by the log–probability plot method.

2.4. Lung deposition model

Deposition of aerosol particles in the human respiratory system was calculated by an advanced version of the stochastic lung deposition model IDEAL (Koblinger and Hofmann, 1990; Hofmann and Koblinger, 1992). Its status among the other particle deposition models was discussed by Asgharian et al. (2009) and Hofmann (2011). For modelling purposes, the respiratory tract is divided into an extra-thoracic (ET, or oro-nasopharyngeal) region, tracheobronchial (TB) tree and acinar (AC) region. The deposition of submicrometer particles in the ET region is modelled by semi-empirical equations derived by Hofmann and Koblinger (1992). The TB tree and AC region are modelled by a sequence of cylindrical tubes asymmetrically branching into two daughter airways. These regions are considered to be made up by a system of bifurcation units, which are composed of half of the parent tube and half of the daughter tubes. In the AC region, in addition to the bifurcations, hemispherical alveoli appear on the walls of the tubes. Proceeding further into the AC region, more and more alveoli cover the walls of the tubes. The respiratory tract is eventually terminated by an alveolar sac, which is completely covered by alveoli. In the stochastic lung model, the path of an inhaled particle through the series of bifurcations is selected randomly by Monte Carlo methods, and the particle follows the same path during expiration.

In the present study, particle deposition was calculated for a Caucasian-type healthy adult female performing reference levels of physical activity. The morphological airway parameter values of the model were selected from the statistical distributions derived from the data of Raabe et al. (1976) in the case of the TB region, and from the Haefeli-Bleuer and Weibel model (1988) in the case of the acinar region, constrained by statistical relationships between some of the parameters. The physiological parameters utilised were chosen according to Hofmann and Koblinger (1990) and the recommendations of the ICRP (1994). Tidal volumes characteristic of sleeping, sitting, light exercise and heavy exercise breathing conditions (i.e., 444, 464, 992 and 1364 cm^3, respectively) were adopted, and the breathing cycle times utilised were 5.0, 4.3, 2.9 and 1.8 s, respectively. It was further assumed for heavy exercise that the fraction of the total ventilatory airflow passing through the nose is 50%, and that the rest is inhaled through the mouth (ICRP, 1994). Deposition fractions (ratios of the number of deposited particles to the total number of inhaled particles) in each airway generation were determined by simulating the route and fate of 100,000 inhaled particles in each computations. Deposition rates (number of deposited particles in a unit time) in each airway generation were calculated from deposition fraction, atmospheric particle number concentration, breathing volume and breathing frequency. Mean surface areas of each airway generation were also computed (Salma et al., 2002b; Balásházy et al., 2007), and were utilised for obtaining deposition rates per unit surface area during unit time, i.e., surface density deposition rates. Finally, it was estimated that the individual deposition data are subject to relative uncertainty smaller than 25% of the computed values.

3. Results and discussion

3.1. Particle size distributions

The median particle number size distributions expressed in the d_{mob} representation are shown separately for the four urban

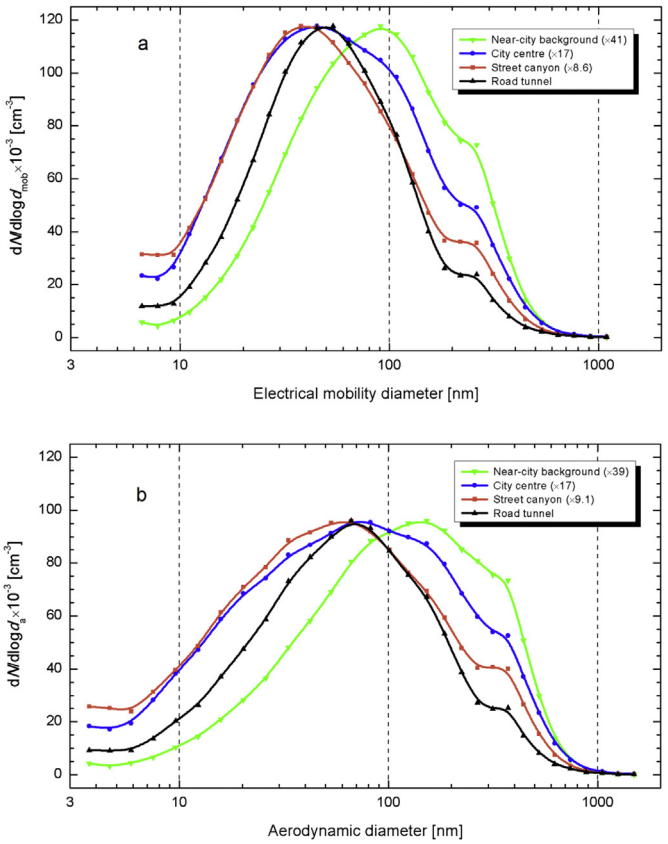

Fig. 1. Median particle number size distributions of atmospheric aerosol particles expressed in electrical mobility diameter (a), and in aerodynamic diameter (b) for the near-city background, city centre, street canyon and road tunnel urban environments. Three curves in each figure were scaled up to the maximal value by factors displayed in brackets to visualize better their shape.

environments in Fig. 1a, while the distributions converted into the d_a representation are displayed in Fig. 1b. Obtaining representative, i.e., average size distributions involves inherent disadvantages due to the significant broadening of the Aitken and accumulation modes, which are generally present in the particle number size distributions. This yielded that the two modes merged into a single wide peak in the average size distributions. The total particle number concentration for the near-city background, city centre, street canyon and road tunnel obtained by summing the channel contents were 2.9×10^3, 8.1×10^3, 14.4×10^3 and 103×10^3 cm^{-3}, respectively for both representations. In the order of the urban environments listed, the NMMDs were 70, 42, 35 and 42 nm, respectively, and the GSDs were between 2.6 and 2.9. The shoulder of the curves at about 200 nm is an artefact, which was caused by switching the flow and high voltage parameters simultaneously in the DMPS system. Its extent usually remains below 10%. The NMMDs imply decreasing tendency with fresh vehicle emissions. The road tunnel is an exception since the particle size distributions there were influenced by a ventilation facility which introduces aged aerosol from the city centre (urban background) into the tunnel, and this contains larger particles than freshly emitted aerosol (Salma et al., 2011b). The NMADs of the distributions were somewhat larger, i.e., 79, 51, 42 and 47 nm, respectively.

According to our simulation results, deposition fractions of particles due to the diffusion mechanism becomes similar to those due to the impaction mechanism at 400–500 nm, depending on the physical activity. This suggests that the size distributions expressed in d_{mob} representation characterise the real deposition behaviour of the particles well for most of the diameter interval considered, and that the size distributions related to the d_a only play a role in a much smaller size interval on the right side of the peaks. Comparative calculations were completed by using the d_{mob} and corresponding d_a in order to examine the sensitivity of the deposition results to switching between these two diameter representations. Deposition fractions in the characteristic regions and whole respiratory tract of an adult woman as a function of the size channel number of the DMPS system are presented in Fig. 2. Median electrical mobility diameters for the 30 size channels varied from 6.55 to 1092 nm, while the corresponding median aerodynamic diameters for the same size channels changed from 3.71 to 1492 nm. (All individual values are displayed in Fig. 1.) Fig. 2 demonstrates that in the diameter interval in which the impaction plays a more important role than the diffusion (size channels approximately from 23 to 30), the differences between the two deposition curves were rather small in the TB and AC regions. Using the d_{mob} representation somewhat underestimates deposition in the ET region, and as a consequence, in the whole respiratory tract with respect to the d_a representation for these particular particle sizes where the impaction dominates the deposition. The differences, however, remained within the uncertainty of the modelled data and inter-subject variability, although they cause a systematic shift. More importantly, the median size distributions ordinary represent small values in this diameter interval. Considering all this, the subsequent computations were conducted by using the particle size distributions in the d_{mob} representation.

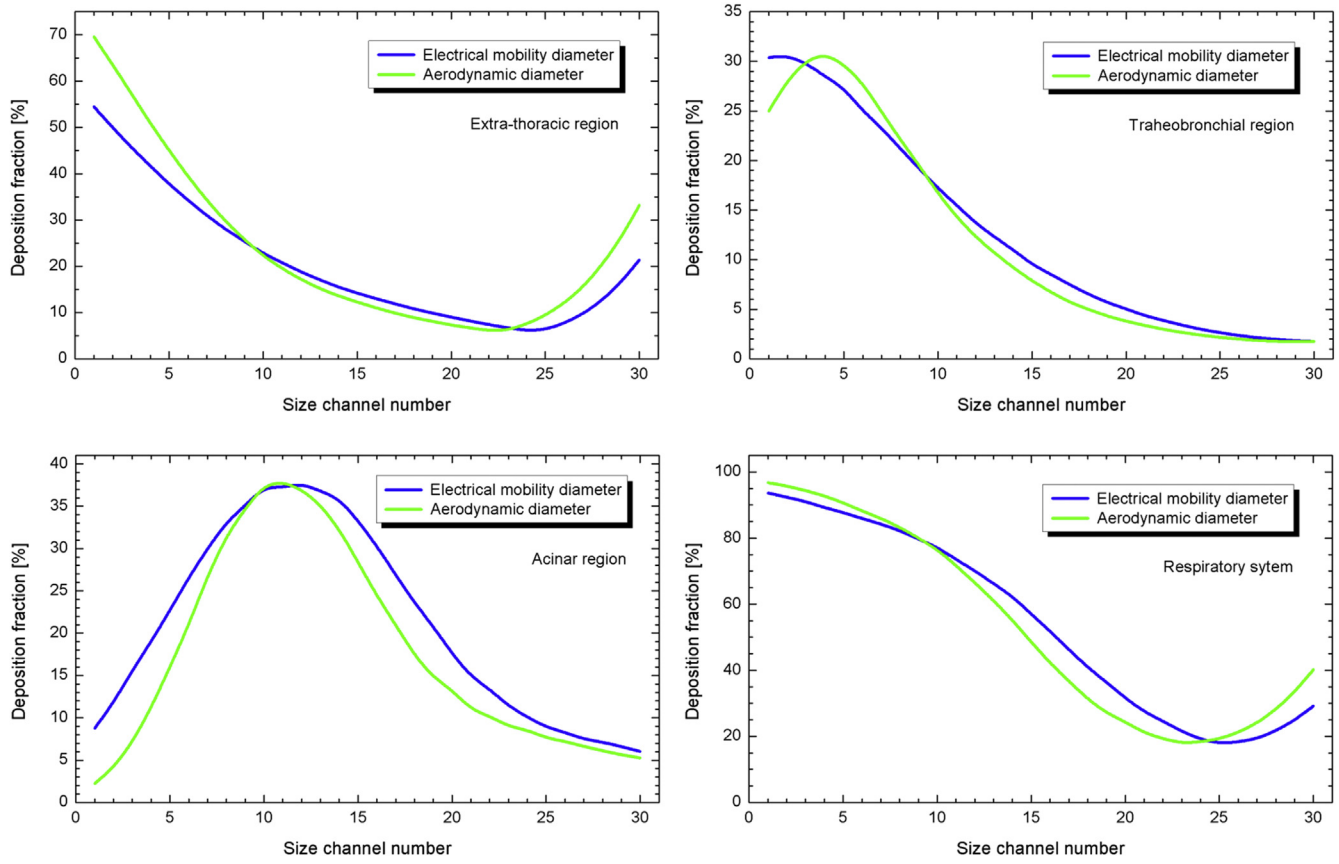

Fig. 2. Deposition fractions of aerosol particles in the extra-thoracic, tracheobronchial and acinar regions, and in the whole respiratory system of an adult woman performing sitting activity calculated by using electrical mobility diameters and corresponding aerodynamic diameters.

3.2. Regional deposition fractions

Deposition fractions of atmospheric aerosol particles in the characteristic regions and total respiratory tract of an adult woman performing reference levels of physical activity in the urban environments are summarized in Table 1. The deposition fractions typically varied by (4–5)% with urban environments at a fixed physical activity, while they commonly changed by (14–19)% with physical activity at a fixed location. It was found that the deposition in the total respiratory tract was considerable and quite constant; its individual values ranged from 46% to 64% with an overall mean and standard deviation of (56 ± 6)%. The mean deposition fractions in the ET region averaged separately for each urban site, together with its standard deviation for sleeping, sitting, light exercise and heavy exercise breathing conditions were (26 ± 3)%, (25 ± 3)%, (18 ± 2)% and (9.4 ± 1.3)%, respectively. The decrease of extra-thoracic deposition with breathing intensity can be explained by the shorter residence times of the particles in the ET region at higher physical activities, and by the assumed 50% contribution of mouth breathing for heavy exercise breathing conditions, which has lower deposition efficiencies. This tendency proofs that the deposition was indeed mainly diffusion driven and not impaction controlled. The corresponding mean deposition fractions in the lung with standard deviations for sleeping, sitting, light exercise and heavy exercise breathing conditions were (28 ± 1)%, (28 ± 1)%, (41 ± 3)% and (45 ± 5)%, respectively. The mean deposition fractions in the TB region averaged separately for each urban site were constant for all physical activities with an overall mean and standard deviation of (12.5 ± 0.7)%, while the corresponding mean deposition fraction and standard deviation for the AC region increased monotonically with physical activity from (14.7 ± 0.6)% for sleeping, to (15.5 ± 0.7)% for sitting activity, to (29 ± 2)% for light exercise and to (34 ± 3)% for heavy exercise. Because of these two dependences, the mean deposition in the AC region averaged separately for each urban site for sleeping, sitting activity, light exercise and heavy exercise contributed to the deposition fraction in the lung with increasing tendency, i.e., by 53%, 55%, 70% and 75%, respectively with standard deviations of approximately 3%.

The deposition fractions for particle numbers (which is mainly determined by nano- and ultrafine particles) in the ET region (7.5%–30%) obtained in the present study are smaller than deposition fractions for particulate mass (which is mainly determined by micrometer-sized particles) derived previously (Salma et al., 2002a, 2002b), which was typically between 43% and 78% at the same urban environments and under similar modelling conditions, while in the TB region (for particle numbers, 8.6%–15%) and AC region (for particle numbers, 14%–36%), they are larger than for aerosol mass, which were approximately between 2.0% and 5.7%, and between 3.3% and 7.2%, respectively. Furthermore, there are also important differences in the tendencies. In contrast to particle numbers of nano- and ultrafine particles, the deposition in the ET region for particulate mass (mainly determined by micrometer-sized particles) increased with rising physical activity, which can be explained by the large (>≈50%) relative contribution of the coarse mode in the mass size distributions. Deposition of the coarse particles (influenced significantly by impaction mechanism) is enhanced by larger respiratory flows (physical activity).

3.3. Regional deposition rates

It is worth mentioning that the total number of particles inhaled in a minute time interval by an adult woman varied from 15×10^6 particles corresponding to sleeping breathing mode in the near-city background to 4.7×10^9 particles while performing heavy exercise in the tunnel. The deposition rates of atmospheric aerosol particles in the characteristic regions and total respiratory tract of an adult woman in the urban environments for the various reference levels of physical activity are shown in Table 2. The values increased monotonically with both the atmospheric concentrations at the urban sites and physical activity. It was found that the total number

Table 1
Deposition fractions of atmospheric aerosol particles in the extra-thoracic, bronchial and acinar regions, in the lung, and in the total respiratory tract of an adult woman for sleeping, sitting, light exercise and heavy exercise breathing conditions in the near-city background, city centre, street canyon and road tunnel urban environments.

Urban site/ respiratory region	Sleeping [%]	Sitting activity [%]	Light exercise [%]	Heavy exercise [%]
Background/				
Extra-thoracic	22	21	14.9	7.5
Bronchial	10.7	10.4	10.0	8.6
Acinar	14.5	15.0	27	30
Lung	25	25	37	38
Total	47	46	52	46
City centre/				
Extra-thoracic	28	26	19.1	10.0
Bronchial	13.4	13.2	13.3	12.0
Acinar	14.3	15.1	29	34
Lung	28	28	42	46
Total	55	55	61	56
Street canyon/				
Extra-thoracic	30	28	21	10.5
Bronchial	14.5	14.2	14.3	13.2
Acinar	14.4	15.3	29	35
Lung	29	30	44	49
Total	58	58	64	59
Road tunnel/				
Extra-thoracic	27	26	18.8	9.5
Bronchial	13.6	13.2	13.2	11.7
Acinar	15.7	16.4	31	36
Lung	29	30	44	48
Total	56	56	62	57

Table 2
Deposition rates of atmospheric aerosol particles expressed in number of particles deposited per minute in the extra-thoracic, bronchial and acinar regions, in the lung, and in the total respiratory tract of an adult woman in the near-city background, city centre, street canyon and road tunnel urban environments for sleeping, sitting, light exercise and heavy exercise breathing conditions.

Physical activity/ respiratory region	Background [10^6 min^{-1}]	City centre [10^6 min^{-1}]	Street canyon [10^6 min^{-1}]	Road tunnel [10^6 min^{-1}]
Sleeping/				
Extra-thoracic	3.3	11.8	23	148
Bronchial	1.64	5.8	11.1	75
Acinar	2.2	6.2	11.0	86
Lung	3.9	12.0	22	161
Total	7.2	24	45	309
Sitting activity/				
Extra-thoracic	3.9	13.8	27	173
Bronchial	1.94	6.9	13.4	88
Acinar	2.8	8.0	14.4	110
Lung	4.7	14.9	28	198
Total	8.6	29	54	371
Light exercise/				
Extra-thoracic	8.9	32	62	402
Bronchial	6.0	22	43	280
Acinar	16.1	48	87	654
Lung	22	71	131	934
Total	31	103	192	1336
Heavy exercise/				
Extra-thoracic	9.8	37	69	444
Bronchial	11.2	44	87	547
Acinar	2.2	6.2	11.0	86
Lung	50	169	319	2226
Total	60	206	388	2670

of particles deposited in the respiratory tract per minute time interval changed dynamically, i.e., from 7.2×10^6 min^{-1} for sleeping in the near-city background to 2.7×10^9 min^{-1} for heavy exercise in the tunnel. All regional deposition rates increased monotonically and substantially (about 130 times for the ET region, 330 times for the TB region, and 750 times for the AC region) in the order of the urban environments: near-city background, city centre, street canyon and road tunnel. This was primarily caused by different atmospheric concentrations at the four urban sites. Ratios of the deposition rate for an urban site to that for the near-city background (to the cleanest location), however, showed a uniform dependency. Mean ratios averaged for physical activities and then for the characteristic respiratory regions, with their standard deviations for the city centre, street canyon and road tunnel were 3.4 ± 0.3, 6.5 ± 0.6 and 44 ± 3, respectively. The ratios were larger by a mean and standard deviation of 1.3 ± 0.3 than the corresponding ratios of particle number concentrations for the urban sites. This suggests indirectly that the increments in the deposition rate were mainly caused by the actual atmospheric concentrations, and that the differences in the particle size distributions at the urban sites contributed to the excess increase by approximately 30%. The exact contribution can, however, depend on the actual environment (size distribution).

Ratios of the deposition rate for a physical activity to that for sleeping averaged for all urban sites were uniform for any characteristic respiratory region, and indicated that it is the deposition in the AC region that was most affected by the physical activity. The mean lung-to-ET deposition rate ratios averaged separately for each site with their standard deviation for sleeping, sitting activity, light exercise and heavy exercise were 1.06 ± 0.09, 1.13 ± 0.08, 2.3 ± 0.2 and 4.8 ± 0.3, respectively. This means that deposition rates in the ET region were smaller than in the lung, and that the deposition rates in the ET region had a decreasing effect on particle removal with physical activity. At the same time, the mean AC-to-TB deposition rate ratios for sleeping, sitting activity, light and heavy exercise averaged for the urban environments were 1.14, 1.23, 2.3 and 3.0 with a relative uncertainty below 13%. This means that the deposition rate in the lung was increasingly realised in the AC region by physical activity. A considerable fraction of the deposited particles can be soluble in the epithelial fluid, which decreases the toxicological hazard, while the insoluble rest of the deposited particles may be phagocytised by alveolar macrophages. In this respect, it is important to mention that the maximum number of macrophages available in the alveolar pool is 2.5×10^7 (Stöber et al., 1994), which suggests that the efficiency of the main clearance mechanism in the AC region is limited by the huge number of deposited particles - even if a macrophage can phagocytise more particles.

Table 3
Surface density deposition rates of atmospheric aerosol particles expressed in number of particles deposited per cm^2 of epithelial area and per minute in the extra-thoracic, bronchial and acinar regions, and in the whole lung of an adult woman in the near-city background, city centre, street canyon and road tunnel urban environments for sleeping, sitting, light exercise and heavy exercise breathing conditions.

Physical activity/ respiratory region	Background [cm^{-2} min^{-1}]	City centre [cm^{-2} min^{-1}]	Street canyon [cm^{-2} min^{-1}]	Road tunnel [cm^{-2} min^{-1}]
Sleeping/				
Extra-thoracic	7,280	26,220	50,300	328,500
Bronchial	610	2,153	4,137	28
Acinar	1.51	4.2	7.5	58
Lung	2.6	8.1	15.2	108
Sitting activity/				
Extra-thoracic	8,520	30,610	58,710	383,300
Bronchial	722	2,580	4,963	32,886
Acinar	1.90	5.4	9.7	74
Lung	3.2	10.1	18.7	134
Light exercise/				
Extra-thoracic	19,730	71,370	136,740	890,000
Bronchial	2,233	8,329	16,000	104,134
Acinar	11	33	59	443
Lung	15.0	48	88	632
Heavy exercise/				
Extra-thoracic	21,690	81,350	145,000	930,900
Bronchial	4,175	16,414	32,227	203,288
Acinar	26	85	158	1,139
Lung	34	114	216	1,510

3.4. Regional surface density deposition rates

The surface density deposition rates of particles in the characteristic regions of the respiratory tract of an adult woman in the four urban environments and for the reference levels of physical activity are presented in Table 3. The values increased monotonically with both urban environments (atmospheric concentrations) and physical activity. The ET region (expectedly the nose) received larger surface density deposition rates by approximately 3 orders of magnitude than the lung. (The mean factor averaged for the urban sites varied from 6.6×10^2 for heavy exercise to 3.1×10^3 for sleeping with relative uncertainties below 7%.) This can be explained by the increased mean free path of the UF particles, and by the special morphology of the nose (narrower and longer airway). If the deposited insoluble nanoparticles cross the cellular membrane in the nose then the question can be raised whether they - especially the hydrophobic particles (Krol et al., 2013), which can make a large portion of the insoluble particles - may partially escape the blood–brain barrier and represent a specific risk for the central nervous system, or alternatively, whether they can find promising applications in clinical neuroscience.

At the same time, the surface density deposition rates for the TB region were also substantially larger than for the AC region. The mean TB-to-AC ratio (averaged for the four urban environments) and corresponding standard deviation for sleeping, sitting activity, light exercise and heavy exercise were 489 ± 64, 453 ± 56, 241 ± 29 and 184 ± 20, respectively. The reason for the decreasing tendency is that more nano- and ultrafine particles reach the AC region by increasing the physical activity. Table 3 also confirms that after deposition of the particles, the agglomeration can be neglected in any characteristic region of the respiratory tract since the probability of two nanoparticles landing on each other is very small.

3.5. Differential deposition fractions

The deposition fractions of atmospheric aerosol particles in the airway generations of an adult woman performing reference levels of physical activity in the urban environments are displayed in Fig. 3. The curves exhibited a single distinct peak, which was realised in the AC region. The maximum of the curves for sleeping, sitting activity, light exercise and heavy exercise occurred at increasing airway generation number, i.e., in generations 17, 17, 19 and 20–21, respectively for all urban environments. The range of the affected airway generations became somewhat larger with physical activity, which means that the aerosol particles penetrated deeper into the lung with increasing physical activity. The differential deposition in the TB region had similar shape and extent for all urban sites.

The shape of the deposition fraction curves for particle numbers showed some obvious differences when compared to the deposition fraction curves of particulate mass, which is mainly determined by micrometer-sized particles (Salma et al., 2002b). In the latter case, the deposition fractions in the TB region contributed to a

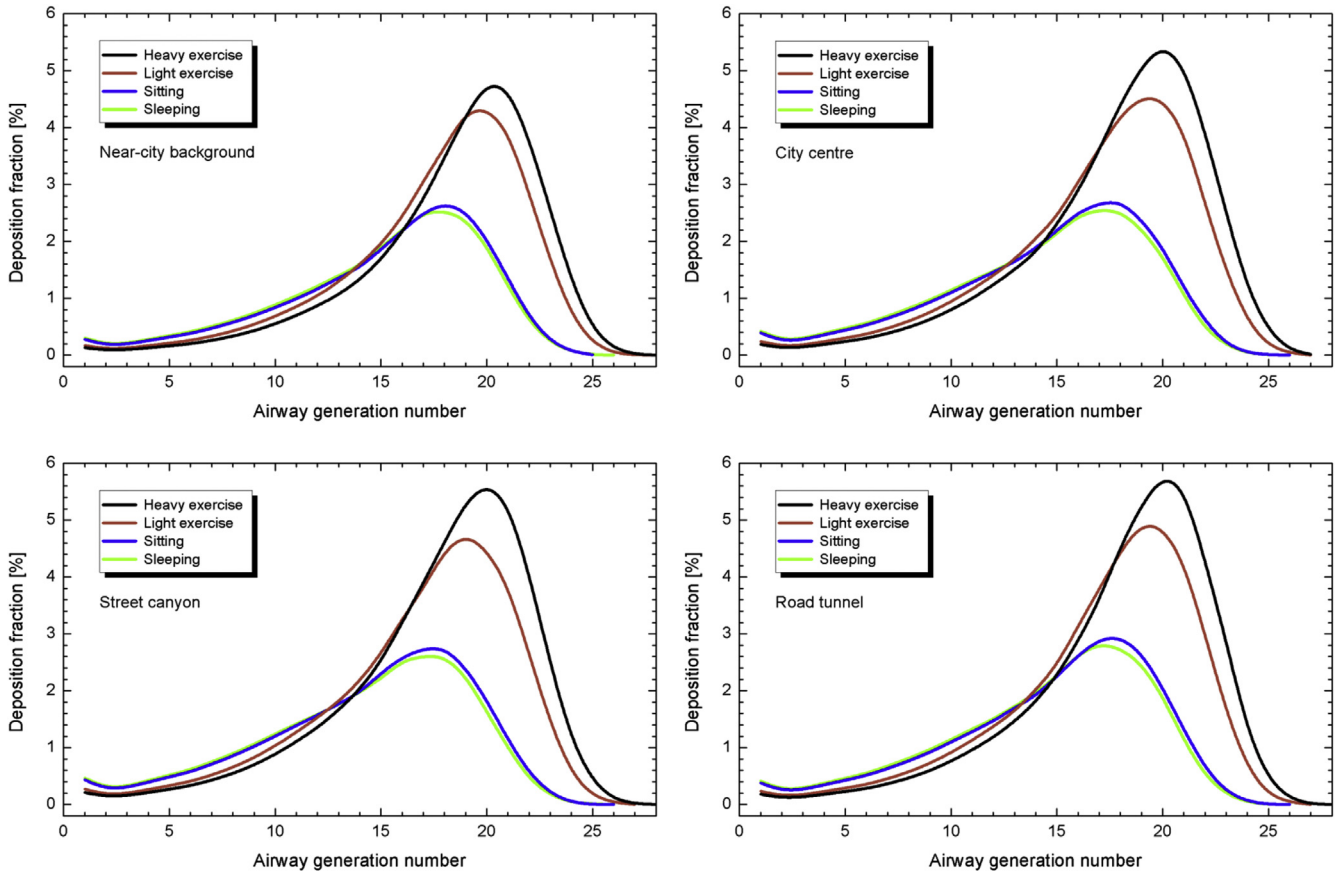

Fig. 3. Deposition fractions of atmospheric aerosol particles in the airway generations of an adult woman in the near-city background, city centre, street canyon and road tunnel urban environments for sleeping, sitting activity, light exercise and heavy exercise.

considerable extent to total deposition, and its share increased substantially with physical activity. This even yielded a new (second) deposition peak in the region of airway generations 12–13. The tendency was completely missing for the particle numbers; deposition fractions in the TB region were modest and constant (if not decreasing) for all physical activities.

3.6. Differential depositions rates

The deposition rates of atmospheric aerosol particles in the airway generations of an adult woman performing reference levels of physical activity in the urban environments are displayed in Fig. 4. These curves also showed a major single peak, and they lined up monotonically in the order of 1) increasing physical activity due to the increased ventilation rates; and 2) urban sites which was primarily caused by different associated atmospheric concentrations. The curves for sleeping and sitting activity were again similar both in shape and magnitude for each urban site, but their maximum changed by an approximate factor of 40 from the near-city background to the road tunnel. The maximum deposition rates for various physical activities appeared in higher airway generations, similar to the differential deposition fraction curves. In the most loaded airway generation (number 20), 266×10^6 particles were deposited per minute in the road tunnel. The slightly increased deposition rate in the first airway generation can be explained with the longer length of the trachea relative to the other bifurcation units.

3.7. Differential surface density deposition rates

The surface density deposition rates of atmospheric aerosol particles in the airway generations of an adult woman in the urban environments for the reference levels of physical activity are displayed in Fig. 5. The shapes of these curves are completely different from the trends observed above. It was the second and third airway generations that received the highest surface loading of particles. This maximum can be explained by fact that the epithelial surface available for deposition is smallest in airway generations 2–4. This tendency is consistent with that for the particulate mass presented earlier (Salma et al., 2002b). In contrast, however, the relative importance of the surface deposition rate of particle number in the airway generation 1 (trachea) does not increase with physical activity, even if mouth breathing takes place. The reason for this phenomenon is that the present process concerns the deposition of nano- and ultrafine particles, which is diffusion controlled, and, therefore, the deposition decreases with physical activity.

The maximum of the curves and the values for the first few airway generations increased uniformly and monotonically with physical activity, by factors of 4.0 for sitting, 7.8 for light exercise and 50 for heavy exercise breathing conditions relative to that for sleeping. The large surface density loading in generations 2 and 4 may be related to the aggravation of upper respiratory illnesses and to lung tumours, which arise primarily in segmental and subsegmental bronchi (ICRP, 1994; Balásházy et al., 2003).

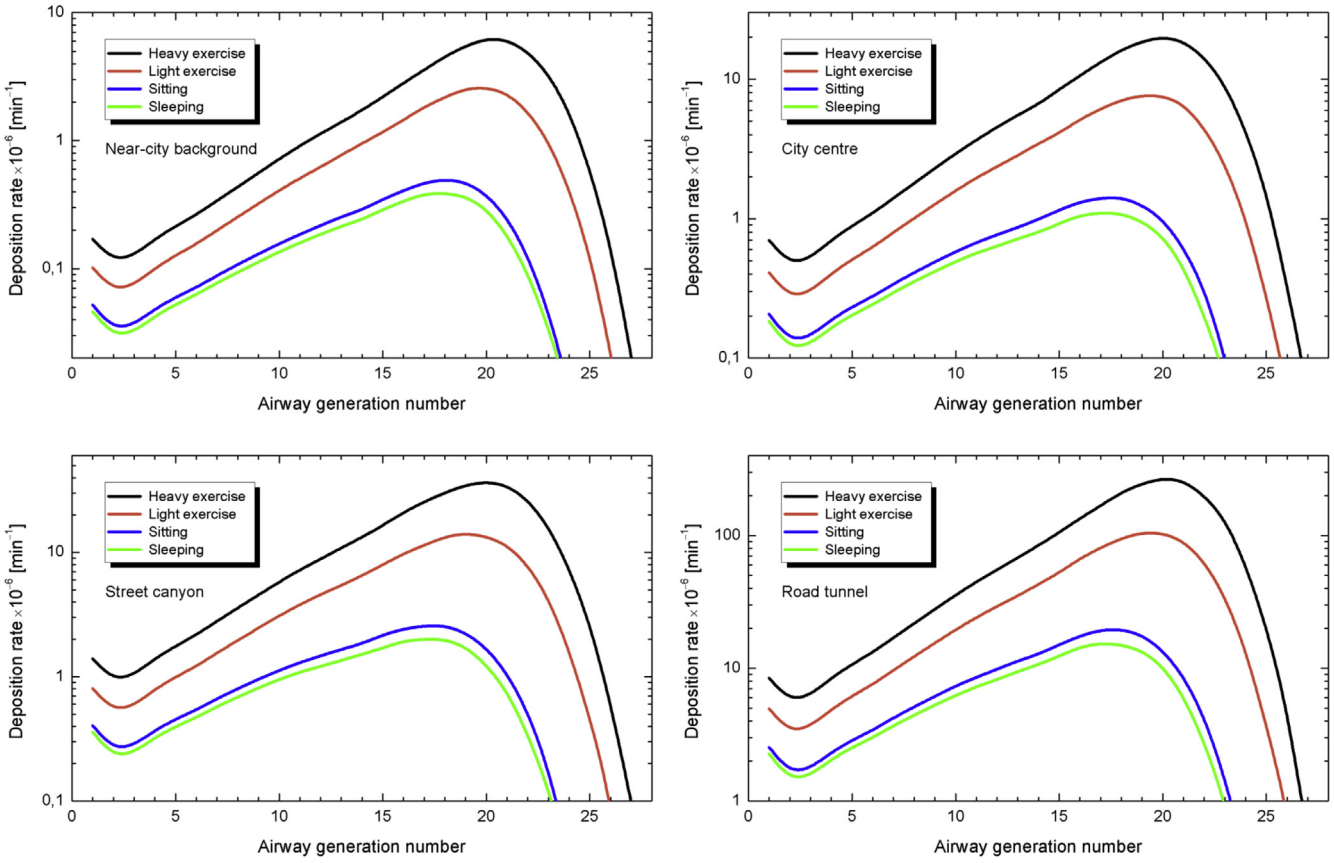

Fig. 4. Deposition rates of atmospheric aerosol particles in the airway generations of an adult woman in the near-city background (with a particle number concentration of 2.9×10^3 cm^{-3}), city centre (8.1×10^3 cm^{-3}), street canyon (14.4×10^3 cm^{-3}) and road tunnel (103×10^3 cm^{-3}) urban environments for sleeping, sitting activity, light exercise and heavy exercise.

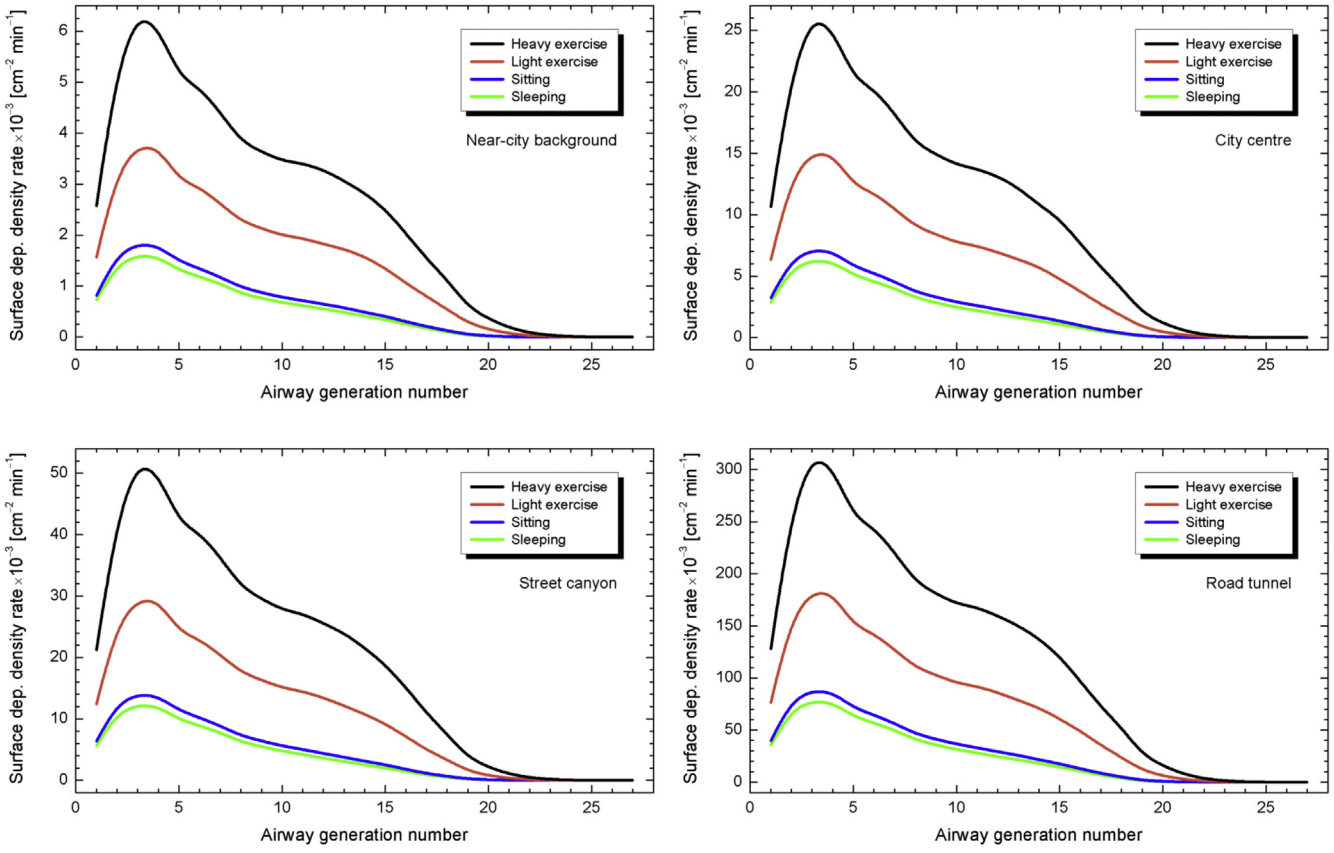

Fig. 5. Surface density deposition rates of atmospheric aerosol particles in the lung of an adult woman in the near-city background (with a particle number concentration of 2.9×10^3 cm^{-3}), city centre (8.1×10^3 cm^{-3}), street canyon (14.4×10^3 cm^{-3}) and road tunnel (103×10^3 cm^{-3}) urban environments for sleeping, sitting activity, light exercise and heavy exercise.

3.8. Normalised differential deposition rates

In order to separate the average effect of the size distribution from the average effect of the particle number concentration, the differential deposition rates and differential surface density deposition rates were normalised to the associated atmospheric particle number concentrations. The airway generation-specific normalised deposition rates (Fig. 6a) and surface density deposition rates (Fig. 6b) in an adult woman performing sitting activity in the urban environments are displayed as illustrative examples. Both types of the curves in Fig. 6 have a distinct peak as expected. The peaks are in the airway generations 17–18 for the deposition rate, and, in the airway generations 2–4 (in the large central airways) for surface density deposition rate. This essential difference has very important health consequences. The local burden (burden in the dimension of a cell environment) has a significant peak in the large central airways even if uniform deposition within the surface of a central airway bifurcations is supposed. In reality, the deposition is far inhomogeneous, which further increases the local cellular burden in the carina of these bifurcations (Balásházy and Hofmann, 2000, 2009). Thus, ultrafine aerosol particles can cause lung cancer (and preneoplastic and neoplastic lesions) preferentially in the carina of airway generations 2–4 in case of radon progeny exposures.

The maxima of the normalised deposition rate curves (Fig. 6a) were shifted monotonically in accordance with the tendency in the median particle diameters for the size distributions (see Fig. 1a). At the same time, there was no obvious or monotonic shift in the peaks of the differential surface density deposition rate curves (Fig. 6b). Instead, it can be seen that the smaller the median particle diameter of the corresponding size distribution, the larger the relative surface density deposition rate. The explanation is related to the differences in the particle size distributions, and to the larger mean free path of smaller particles. Furthermore, the differences in the curves in Fig. 6b for the different urban environments seemed to be larger than those in Fig. 6a, which implies that the surface density deposition rates appeared to be more sensitive to the changes in the size distributions than the deposition rates. This emphasizes again that variations in both the atmospheric concentrations and particle size distributions (median diameters) should be jointly taken into consideration when assessing potential exposure and toxic effects of inhaled UF particles.

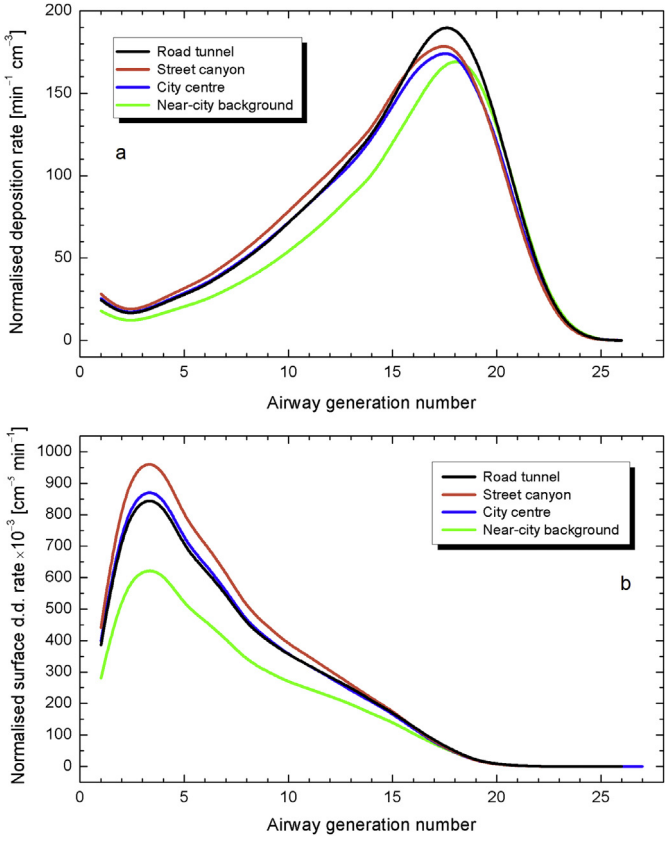

Fig. 6. Normalised deposition rates (a) and normalised surface density deposition rates (b) of atmospheric aerosol particles in the airway generations of an adult woman for sitting activity in the near-city background (with a particle number concentration of 2.9 × 10^3 cm^{-3}), city centre (8.1 × 10^3 cm^{-3}), street canyon (14.4 × 10^3 cm^{-3}) and road tunnel (103 × 10^3 cm^{-3}) urban environments. The curves were normalised to the associated particle number concentrations.

4. Conclusions

In the present study, the attention was focused on the exposure of a healthy adult female. The respiratory tract of an adult male approaches that for a female. Our preliminary computations indicated that in the case of a male, the ET deposition fractions of the polydisperse urban nano- and UF particles are smaller by (10–15)% than for a female depending mainly on the physical activity. At the same time, the deposition fractions in the TB region are larger by approximately 10%, and they are larger by ca. 50% in the AC region than for a female. As a consequence, the deposition fraction in the total respiratory tract of a male is larger by approximately 35% than of a female. The main reason for the differences is the higher ventilation velocity in the lung of a male. The deposition rate in the total respiratory tract increases by about 50% for a male in comparison to a female. The lung of a child differs significantly from that for adults in terms of airway dimensions and breathing rates (Ménache et al., 2008). Due to the combination of smaller airway sizes, smaller tidal volumes, but higher breathing frequencies, the total deposition fraction in children, particularly in infants, is generally higher than that in adults (Asgharian et al., 2004). Thus children may be of a greater health risk from exposure to urban aerosol because of the increased deposition as well as higher sensitivity to air pollutants (WHO, 2005). This emphasizes the need for the research devoted to this direction.

Aerosol particles in this work were characterised by their dry equivalent diameter. There is little information available yet on the interaction of urban type UF particles with water vapour at various RHs. It is thought that part of them (e.g., soot particles) is hydrophobic, which are expected to show little change in their size during inhalation. Another part of them can grow rapidly at RHs present in the airways, which can be larger than in the ambient air (Varghese and Gangamma, 2009). In case of hygroscopic growth factors of 2, which is a typical value for atmospheric aerosol, the shift to larger particle diameters would reduce the deposition fractions and related densities predicted in this paper by a factor of approximately 1.6 (Winkler et al., 2014). Hygroscopic growth properties should be determined for ambient urban UF particles in order to obtain more detailed results and conclusions.

In the current model, uniform deposition of particles within bifurcation units was assumed. It was, however, demonstrated previously (Balásházy et al., 2003) that accumulation of monodisperse particles by up to 2–3 orders of magnitude can occur in the carina of bifurcation units (in hot-spots) relative to the airway walls for particles that are deposited mainly by inertial impaction mechanism. Further studies with realistic polydisperse urban aerosol are desired to improve our knowledge on detailed local distributions of nanoparticles within a bifurcation unit or oro-nasopharyngeal region caused by diffusion controlled deposition

mechanism.

The present research also showed that realistic ambient atmospheric aerosol - that ordinary persists in the air in cities - contains particles with a diameter between 20 and 200 nm in the largest abundance. Thus, the exposure to the ambient nanoparticles (d < 10 nm) is usually limited, since their colloidal system is thermodynamically not stable, and most of them are removed from the air by atmospheric processes (e.g., agglomeration of primary particles, coagulation, scavenging, ageing processes) during a reasonable time interval (<several hours) under ordinary ambient conditions. The exposure to engineered nanoparticles in the indoors or closed spaces, in particular close to their sources, and to specific aerosol particles that have electrical surface charge or repelling coatings can be different.

Finally, important differences in the respiratory locations, magnitudes of and some tendencies in particle deposition can occur when different aerosol metrics are considered. Different size distributions have different average diameters, which generate different deposition patters in the respiratory tract since the deposition efficiencies are size dependent. As there is no general consensus on which aerosol property or chemical component, if any at all, may be responsible for adverse health effects of particles (e.g., Giechaskiel et al., 2009), the next modelling evaluations should involve particle surface area or accessible deposited surface area size distributions as well.

Acknowledgements

Financial support by the Hungarian Scientific Research Fund (contract K84091) is appreciated. The study was also supported by the KTIA_AIK_12-1-2012-0019 Hungarian project. The authors thank to P. Ábrahám, director, Gy. Mező and A. Holl, researchers of the Konkoly Observatory of the Hungarian Academy of Sciences for their support during the field measurements at their campus site.

References

Aalto, P., Hämeri, K., Paatero, P., Kulmala, M., Bellander, T., Berglind, N., Bouso, L., Castaño-Vinyals, G., Sunyer, J., Cattani, G., Marconi, A., Cyrys, J., von Klot, S., Peters, A., Zetzsche, K., Lanki, T., Pekkanen, J., Nyberg, F., Sjövall, B., Forastiere, F., 2005. Aerosol particle number concentration measurements in five European cities using TSI-3022 condensation particle counter over a three-year period during health effects of air pollution on susceptible subpopulations. J. Air Waste Manag. Assoc. 55, 1064–1076.

Asgharian, B., Ménache, M.G., Miller, F.J., 2004. Modeling age-related particle deposition in humans. J. Aerosol Med. 17, 213–224.

Asgharian, B., Price, O., Miller, F., Subramaniam, R., Cassee, F.R., Freijer, J., van Bree, L., Winter-Sorkina, R., 2009. Multiple-path Particle Dosimetry Model (MPPD v. 2.11): a Model for Human and Rat Airway Particle Dosimetry. Applied Research Associates, Hamner Institutes for Health Sciences, National Institute for Public Health and the Environment, and Ministry of Housing, Spatial Planning and the Environment, Raleigh, North Carolina, USA.

Avino, P., Casciardi, S., Fanizza, C., Manigrasso, M., 2011. Deep investigation of ultrafine particles in urban air. Aerosol Air Qual. Res. 11, 654–663.

Balásházy, I., Hofmann, W., 2000. Quantification of local deposition patterns of inhaled radon decay products in human bronchial airway bifurcations. Health Phys. 78, 147–158.

Balásházy, I., Hofmann, W., Heistracher, T., 2003. Local particle deposition patterns may play a key role in the development of lung cancer. J. App. Physiol. 94, 1719–1725.

Balásházy, I., Alföldy, B., Molnár, A.J., Hofmann, W., Szőke, I., Kis, E., 2007. Aerosol drug delivery optimization by computational methods for the characterization of total and regional deposition of therapeutic aerosols in the respiratory system. Curr. Computer-Aided Drug Des. 3, 13–32.

Balásházy, I., Farkas, Á., Madas, B.G., Hofmann, W., 2009. Non-linear relationship of cell hit and transformation probabilities in low dose of inhaled radon progenies. J. Radiol. Prot. 29, 147–162.

Borsós, T., Řimnáčová, D., Ždímal, V., Smolík, J., Wagner, Z., Weidinger, T., Burkart, J., Steiner, G., Reischl, G., Hitzenberger, R., Schwarz, J., Salma, I., 2012. Comparison of particulate number concentrations in three Central European capital cities. Sci. Total Environ. 433, 418–426.

Braakhuis, H.M., Park, M.V., Gosens, I., De Jong, W.H., Cassee, F.R., 2014. Physicochemical characteristics of nanomaterials that affect pulmonary inflammation. Part Fibre Toxicol. 11, 18. http://dx.doi.org/10.1186/1743-8977-11-18.

Carvalho, T.C., Peters, J.I., Williams 3rd, R.O., 2011. Influence of particle size on regional lung deposition–what evidence is there? Int. J. Pharm. 406, 1–10.

Dall'Osto, M., Querol, X., Alastuey, A., O'Dowd, C., Harrison, R.M., Wenger, J., Gómez-Moreno, F.J., 2013. On the spatial distribution and evolution of ultrafine particles in Barcelona. Atmos. Chem. Phys. 13, 741–759.

DeCarlo, P.F., Slowik, J.G., Worsnop, D.R., Davidovits, P., Jimenez, J.L., 2004. Particle morphology and density characterization by combined mobility and aerodynamic diameter measurements. Part 1: Theory. Aerosol Sci. Technol. 38, 1185–1205.

Giechaskiel, B., Alföldy, B., Drossinos, Y., 2009. A metric for health effects studies of diesel exhaust particles. J. Aerosol Sci. 40, 639–651.

Geiser, M., Rothen-Rutishauser, B., Kapp, N., Schürch, S., Kreyling, W., Schulz, H., Semmler, M., Im Hof, V., Heyder, J., Gehr, P., 2005. Ultrafine particles cross cellular membranes by nonphagocytic mechanisms in lungs and in cultured cells. Environ. Health Perspect. 113, 1555–1560.

Geiser, M., Casaulta, M., Kupferschmid, B., Schulz, H., Semmler-Behnke, M., Kreyling, W., 2008. The role of macrophages in the clearance of inhaled ultrafine titanium dioxide particles. Am. J. Respir. Cell. Mol. Biol. 38, 371–376.

Haefeli-Bleuer, B., Weibel, E.R., 1988. Morphometry of the human pulmonary acinus. Anat. Rec. 220, 401–414.

Harrison, R.M., Jones, A.M., 2005. Multisite study of particulate number concentrations in urban air. Environ. Sci. Technol. 39, 6063–6070.

HEI Review Panel on Ultrafine Particles: Understanding the Health Effects of Ambient Ultrafine Particles. HEI Perspectives 3, 2013. Health Effects Institute, Boston, MA.

Hofmann, W., Koblinger, L., 1990. Monte Carlo modelling of aerosol deposition in human lungs. Part II: deposition fractions and their sensitivity to parameter variations. J. Aerosol Sci. 21, 675–688.

Hofmann, W., Koblinger, L., 1992. Monte Carlo modelling of aerosol deposition in human lungs. Part III: comparison with experimental data. J. Aerosol Sci. 23, 51–63.

Hofmann, W., 2011. Modelling inhaled particle deposition in the human lung – a review. J. Aerosol Sci. 42, 693–724.

International Commission on Radiological Protection (ICRP), 1994. Human respiratory tract model for radiological protection. Ann. ICRP 24. Publication 66.

Jeong, C.-H., Evans, G.J., Hopke, P.K., Chalupa, D., Utell, M.J., 2006. Influence of atmospheric dispersion and new particle formation events on ambient particle number concentration in Rochester, United States, and Toronto, Canada. J. Air Waste Manage Assoc. 56, 431–443.

Khlystov, A., Stanier, C., Pandis, S.N., 2004. An algorithm for combining electrical mobility and aerodynamic size distributions data when measuring ambient aerosol. Aerosol Sci. Technol. 38, 229–238.

Koblinger, L., Hofmann, W., 1990. Monte Carlo modeling of aerosol deposition in human lungs. Part I: simulation of particle transport in a stochastic lung structure. J. Aerosol Sci. 21, 661–674.

Kreyling, W.G., Semmler, M., Erbe, F., Mayer, P., Takenaka, S., Schulz, H., Oberdörster, G., Ziesenis, A., 2002. Translocation of ultrafine insoluble iridium particles from lung epithelium to extrapulmonary organs is size dependent but very low. J. Toxicol. Environ. Health A 65, 1513–1530.

Kreyling, W.G., Semmler-Behnke, M., Möller, W., 2006. Ultrafine particle-lung interactions: does size matter? J. Aerosol Med. 19, 74–83.

Krol, S., MacRez, R., Docagne, F., Defer, G., Laurent, S., Rahman, M., Hajipour, M.J., Kehoe, P.G., Mahmoudi, M., 2013. Therapeutic benefits from nanoparticles: the potential significance of nanoscience in diseases with compromise to the blood brain barrier. Chem. Rev. 113, 1877–1903.

Kulmala, M., Vehkamäki, H., Petäjä, T., Dal Maso, M., Lauri, A., Kerminen, V.-M., Birmili, W., McMurry, P., 2004. Formation and growth rates of ultrafine atmospheric particles: a review of observations. J. Aerosol Sci. 35, 143–176.

Ménache, M.G., Hofmann, W., Asgharian, B., Miller, F.J., 2008. Airway geometry: models of children's lungs for use in dosimetry modeling. Inhal. Toxicol. 20, 101–126.

Nel, A., Xia, T., Mädler, L., Li, N., 2006. Toxic potential of materials at the nanolevel. Science 311, 622–627.

Oberdörster, G., Oberdörster, E., Oberdörster, J., 2005. Nanotoxicology: an emerging discipline evolving from studies of ultrafine particles. Environ. Health Perspect. 113, 823–839.

Ondráček, J., Ždímal, V., Smolík, J., Lazaridis, M., 2009. A merging algorithm for aerosol size distribution from multiple instruments. Water Air Soil Pollut. 199, 219–233.

Park, K., Kittelson, D.B., Zachariah, M.R., McMurry, P.H., 2004. Measurement of inherent material density of nanoparticle agglomerates. J. Nanopart Res. 6, 267–272.

Putaud, J.-P., Van Dingenen, R., Alastuey, A., Bauer, H., Birmili, W., Cyrys, J., Flentje, H., Fuzzi, S., Gehrig, R., Hansson, H.C., Harrison, R.M., Herrmann, H., Hitzenberger, R., Hüglin, C., Jones, A.M., Kasper-Giebl, A., Kiss, G., Kousa, A., Kuhlbusch, T.A.J., Löschau, G., Maenhaut, W., Molnár, A., Moreno, T., Pekkanen, J., Perrino, C., Pitz, M., Puxbaum, H., Querol, X., Rodriguez, S., Salma, I., Schwarz, J., Smolik, J., Schneider, J., Spindler, G., ten Brink, H., Tursic, J., Viana, M., Wiedensohler, A., Raes, F., 2010. An European aerosol phenomenology – 3: physical and chemical characteristics of particulate matter from 60 rural, urban, and kerbside sites across Europe. Atmos. Environ. 44, 1308–1320.

Qian, S., Sakurai, H., McMurry, P.H., 2007. Characteristics of regional nucleation events in urban East St. Louis. Atmos. Environ. 41, 4119–4127.

Raabe, O.G., Yeh, H.-C., Schum, G.M., Phalen, R.F., 1976. Tracheo-bronchial

Geometry: Human, Dog, Rat, Hamster – a Compilation of Selected Data from the Project Respiratory Tract Deposition Models. Report LF-53. Lovelace Foundation, Albuquerque, NM.

Reche, C., Querol, X., Alastuey, A., Viana, M., Pey, J., Moreno, T., Rodríguez, S., González, Y., Fernández-Camacho, R., de la Rosa, J., Dall'Osto, M., Prévôt, A.S.H., Hueglin, C., Harrison, R.M., Quincey, P., 2011. New considerations for PM, Black Carbon and particle number concentration for air quality monitoring across different European cities. Atmos. Chem. Phys. 11, 6207–6227.

Rissler, J., Messing, M.E., Malik, A.I., Nilsson, P.T., Nordin, E.Z., Bohgard, M., Sanati, M., Pagels, J.H., 2013. Effective density characterization of soot agglomerates from various sources and comparison to aggregation theory. Aerosol Sci. Technol. 47, 792–805.

Rodríguez, S., Van Dingenen, R., Putaud, J.-P., Dell'Acqua, A., Pey, J., Querol, X., Alastuey, A., Chenery, S., Ho, K.-F., Harrison, R.M., Tardivo, R., Scarnato, B., Gemelli, V., 2007. A study on the relationship between mass concentrations, chemistry and number size distribution of urban fine aerosols in Milan, Barcelona and London. Atmos. Chem. Phys. 7, 2217–2232.

Salma, I., Balásházy, I., Winkler-Heil, R., Hofmann, W., Záray, G.Y., 2002a. Effect of particle mass size distribution on the deposition of aerosols in the human respiratory system. J. Aerosol Sci. 33, 119–132.

Salma, I., Balásházy, I., Hofmann, W., Záray, G.Y., 2002b. Effect of physical exertion on the deposition of urban aerosols in the human respiratory system. J. Aerosol Sci. 33, 983–997.

Salma, I., Borsós, T., Weidinger, T., Aalto, P., Hussein, T., Dal Maso, M., Kulmala, M., 2011a. Production, growth and properties of ultrafine atmospheric aerosol particles in an urban environment. Atmos. Chem. Phys. 11, 1339–1353.

Salma, I., Borsós, T., Aalto, P.P., Kulmala, M., 2011b. Time-resolved number concentration and size distribution of aerosol particles in an urban road tunnel. Boreal Environ. Res. 16, 262–272.

Salma, I., Borsós, T., Németh, Z., Weidinger, T., Aalto, P., Kulmala, M., 2014. Comparative study of ultrafine atmospheric aerosol within a city. Atmos. Environ. 92, 154–161.

Stöber, W., Morrow, P.E., Koch, W., Morawietz, G., 1994. Alveolar clearance and retention of inhaled insoluble particles in rats simulated by a model inferring macrophage particle load distribution. J. Aerosol Sci. 25, 975–1002.

Varghese, S.K., Gangamma, S., 2009. Particle deposition in human respiratory system: deposition of concentrated hygroscopic aerosols. Inhal. Toxicol. 21, 619–630.

Wehner, B., Wiedensohler, A., 2003. Long term measurements of submicrometer urban aerosols: statistical analysis for correlations with meteorological conditions and trace gases. Atmos. Chem. Phys. 3, 867–879.

Wiedensohler, A., Birmili, W., Nowak, A., Sonntag, A., Weinhold, K., Merkel, M., Wehner, B., Tuch, T., Pfeifer, S., Fiebig, M., Fjäraa, A.M., Asmi, E., Sellegri, K., Depuy, R., Venzac, H., Villani, P., Laj, P., Aalto, P., Ogren, J.A., Swietlicki, E., Williams, P., Roldin, P., Quincey, P., Hüglin, C., Fierz-Schmidhauser, R., Gysel, M., Weingartner, E., Riccobono, F., Santos, S., Grüning, C., Faloon, K., Beddows, D., Harrison, R., Monahan, C., Jennings, S.G., O'Dowd, C.D., Marinoni, A., Horn, H.-G., Keck, L., Jiang, J., Scheckman, J., McMurry, P.H., Deng, Z., Zhao, C.S., Moerman, M., Henzing, B., de Leeuw, G., Löschau, G., Bastian, S., 2012. Mobility particle size spectrometers: harmonization of technical standards and data structure to facilitate high quality long-term observations of atmospheric particle number size distributions. Atmos. Meas. Tech. 5, 657–685.

Winkler-Heil, R., Ferron, G., Hofmann, W., 2014. Calculation of hygroscopic particle deposition in the human lung. Inhal. Toxicol. 26, 193–206.

World Health Organization (WHO), 2005. Effects of Air Pollution on Children's Health and Development. Regional Office for Europe, Bonn.

Yang, W., Peters, J.I., Williams 3rd, R.O., 2008. Inhaled nanoparticles – a current review. Int. J. Pharm. 356, 239–247.